Multispectral Detection of Fecal Contamination on Apples Based on Hyperspectral Imagery: Part II. Application of Hyperspectral Fluorescence Imaging

M. S. Kim, A. M. Lefcourt, Y. R. Chen, I. Kim, D. E. Chan, K. Chao

Abstract. *Pathogenic* E. coli *contamination in unpasteurized apple juice or cider is thought to originate from animal feces, and fecal contamination of apples has been recognized by the FDA as an important health issue. In a companion article, reflectance imaging techniques were shown inadequate for the detection of thin smears of feces applied to apples. The objective of this study was to evaluate the use of fluorescence imaging techniques to detect fecal contamination on apple surfaces. A hyperspectral imaging system based on a spectrograph, camera, and UV light source was used to obtain hyperspectral images of Red Delicious, Fuji, Golden Delicious, and Gala apples. Fresh dairy feces were applied to each apple as both a thick patch and as a thin smear. Results indicate that multispectral fluorescence techniques can be used to effectively detect fecal contamination on apple surfaces. Both principal component analysis and examination of emission maxima identified the same four multispectral bands (450, 530, 685, and 735 nm) as being the optimal bands to allow discrimination of contaminated apple surfaces. Furthermore, the simple two–band ratio (e.g., 685 to 450 nm) reduced the variation in normal apple surfaces while accentuating differences between contaminated and uncontaminated areas. Because of the limited sample size, delineation of an optimal detection scheme is beyond the scope of the current study. However, the results suggest that use of multispectral fluorescence techniques for detection of fecal contamination on apples in a commercial setting may be feasible.*

Keywords. *Hyperspectral imaging, Fluorescence, Multispectral imaging, Apples, Fecal contamination.*

On–line sensing using spectral imaging with several spectral bands can provide rapid and non–invasive means to assess agricultural commodities for their quality and safety for human consumption (Abbott et al., 1997; Chen et al., 2002; Throop et al., 1995). In general, these sensing techniques rely on reflectance measurements, in which reflected radiation provided by an illumination source is captured using an imaging or spectroscopic sensor system. The resulting data are analyzed to determine quality or if anomalies are present. Another optical sensing technique that can be implemented on–line is based on fluorescence, in which light absorption at a given wavelength by a compound (chromophore) is followed by the emission of light (normally at longer wavelengths). Steady–state fluorescence techniques are generally regarded as more sensitive optical sensing tools than reflectance techniques, mainly due to greater dynamic responses to changes in compound concentrations, and especially to subtle changes in biological entities. Steady–state fluorescence sensing techniques are widely used in a number of scientific applications including in cell biology, photochemistry, medicine, and environmental sciences (Harris and Hartly, 1976; Hewett et al., 2001; Kim, 1973; Tassetti et al., 1997).

Many natural compounds emit fluorescence when excited with radiation at the proper wavelengths. Plant materials including leaves and fruits exhibit fluorescence emissions in the visible (VIS) region of the spectrum when excited with ultraviolet (UV) radiation (Chappelle et al., 1991; Kim et al., 2001b; Krizek et al., 2001; Sowinska et al., 1998). Fluorescence emission peaks (maxima) from these biological materials are typically observed in the blue, green, red, and far–red regions of the spectrum at approximately 450, 530, 685, and 735 nm, respectively. The blue–green fluorescence is due to multi–compounds in nature, while red and far–red fluorescence emanate primarily from chlorophyll *a* molecules. Animal fecal matter (e.g., cow and deer) emits fluorescence in the same spectral regions as green plant materials when excited with UV radiation (Kim et al., 2001a).

Increasing concerns with food–borne diseases have emerged during the last decade. For instance, pathogenic *E. coli* contamination in unpasteurized apple juice or cider is thought to originate from animal feces (Cody et al., 1999). Undetected, the apple juice industry may use fecal–contaminated apples to produce cider or juice, with potentially deleterious consequences to human health. Fecal contamination of apples has been recognized by the U.S. Food and Drug

Article was submitted for review in February 2002; approved for publication by the Information & Electrical Technologies Division of ASAE in August 2002.

Company and product names are used for clarity and do not imply any endorsement by the USDA to the exclusion of other comparable products.

The authors are **Moon S. Kim,** Research Physicist, **Alan M. Lefcourt, ASAE Member Engineer,** Research Biomedical Engineer, **Yud–Ren Chen, ASAE Member Engineer,** Research Leader, **Diane E. Chan,** Agricultural Engineer, and **Kevin Chao, ASAE Member Engineer,** Research Agricultural Engineer, USDA–ARS Instrumentation and Sensing Laboratory, Henry A. Wallace Beltsville Agricultural Research Center, Beltsville, Maryland; and **Intaek Kim,** Associate Professor, Department of Information Engineering, Myongji University, Yongin, Kyonggido, South Korea. **Corresponding author:** Moon S. Kim, USDA/ARS/ISL, Bldg 303 BARC–East, 10300 Baltimore Ave., Beltsville, MD 20705–2350; phone: 301–504–8450; fax: 301–504–9466; e–mail: kimm@ba.ars.usda.gov.

Administration as an important health issue (FDA, 2001). A companion article describes the use of hyperspectral VIS/near–infrared (NIR) reflectance imaging technique to assess fecal contamination on apple surfaces. Results from the former study suggest that reflectance measurements lack the sensitivity necessary for detection of fecal matter when the contamination on apple surfaces is semi–transparent (not readily visible to the human eye). The objective of this article is to evaluate the use of fluorescence techniques to detect fecal contamination on apple surfaces. More specifically, hyperspectral fluorescence imaging techniques are used to examine spectral features of normal and fecal–contaminated parts and potential multispectral approaches that use a limited number of wavelengths for detection of fecal contamination on apples.

Materials and Methods

Hyperspectral Imaging System

The hyperspectral imaging system developed in our laboratory is a line–by–line scanning system designed to work in the VIS to NIR regions of the spectrum. The key components of the system are a camera, a spectrograph, and a lens along with a sample transport mechanism and appropriate lighting sources. The camera is thermo–electrically cooled and contains a 16 bit, back–illuminated, CCD with 512 × 512 pixels (PixelVision Inc., Tigard, Ore.). The spectrograph (ImSpector–V9, Spectral Imaging, Ltd., Oulu, Finland) is based on prism–grating–prism (PGP) optics and is coupled to an *f* 1.4 C–mount lens (Schneider Optics Inc., Hauppauge, N.Y.). The spectrograph disperses incoming radiation along the scan line into spectral information for each spatial location. Note that not all CCD pixel elements were used in this study. The system typically captures 408 spatial pixels, while no– or 4–pixel binning is used for the spectral dimension, which yields 256 or 128 spectral channels, respectively. For the fluorescence imaging study, only data from the spectrum region from 425 to 752 nm (up to the chlorophyll *a* fluorescence emission band) were used. With 2–pixel binning, this region corresponds to 90 individual spectral channels with approximately 3.6 nm channel interval. The full width at half maximum (FWHM) of the system is approximately 10 nm. The system is equipped with two independent illumination sources for fluorescence and reflectance measurements, respectively.

For fluorescence measurements, two UV–A fluorescent lamp assemblies (Model XX–15A 365 nm, Spectronics Corp., Westbury, N.Y.) are arranged toward the line of IFOV (instantaneous field of view) at 30º backward and forward, to provide near–uniform excitation energy. Short–pass filters (UG1, Schott Glass Technologies, Inc., Duryea, Pa.) placed in front of the lamp housing are used to prevent transmittance of radiations greater than approximately 400 nm and thus eliminate potential spectral contamination by pseudo–fluorescence. A conveyor belt moves sample materials through the line of IFOV in a transverse direction.

Data corrections were performed on raw fluorescence image data to obtain relative fluorescence intensity (RFI) measurements. Individual pixel responses obtained from flat–field fluorescent targets were normalized to the average of all the pixel intensities for each wavelength to correct for heterogeneous spatial responses of the system. Several flat field materials were used to perform this correction. For a detailed description of the ISL hyperspectral imaging system and calibration procedures, refer to Kim et al. (2001c).

Apple Samples and Fecal Contamination

Four cultivars of apples (Red Delicious, Gala, Fuji, and Golden Delicious) were used. To address differences in coloration due to environmental growth conditions, apples were selected to represent the range of green to red colorations. To mimic different possible thickness of fecal contamination, feces were applied to apples as a thick patch or as a thin, semi–transparent smear (not readily visible to the human eye).

Apples were selected from crates of apples that were kept in a cold storage room (2° C to 4° C) after they were harvested the previous season (1999) in Pennsylvania (Rice Fruit Co., Gardners, Pa.). Within each cultivar, individual apples display color variations due mainly to environmental growth conditions such as solar exposure. For instance, sun–exposed apples ripen faster than apples with less exposure to direct solar radiation. Apple sides showing near–uniform color were classified as sun–exposed, while apple sides showing red–green variegations or green color were classified as shaded. Four apples were selected for each of the four cultivars such that the apples represented the full range of normal color variation. A total of 16 apples was used in this study.

Fresh feces were obtained from a pasture at the Beltsville dairy. Two spots of feces were applied to one side of each apple. One spot was a 2 mm thick patch, while the second was a thin, transparent smear. A spatula was used to evenly apply fecal matter on an apple surface to create the thick patch, while a ball of fecal matter was lightly pressed against an apple surface and removed to create the thin smear. Both spots were approximately 1 cm in diameter. For scanning, four treated apples per cultivar were placed on a tray painted with non–fluorescent, flat black paint to minimize background scattering.

Data Processing and Analysis

Software was developed using Visual Basic (Microsoft, Seattle, Wash.) to correct and convert the individual raw data files downloaded from the camera into 16–bit hyperspectral fluorescence (RFI) images. The software includes functions to allow image visualization/enhancement, simple threshold classification, gray–scale image stretch, bands arithmetic operations, and spectral and spatial data retrieval. Processed images or spectra were saved as a standard 8–bit bitmap, ASCII files, and in the data file format required by the commercial software package ENVI (Environment for Visualizing Images, Version 3.2, Research Systems Inc., Boulder, Colo.) for further analysis.

The principle goal of this study was to determine image–processing algorithms that would allow fecal–contaminated surfaces to be differentiated from uncontaminated apple surfaces. The four major aspects of the study were (1) reduction in the size of the spectral dimension of the data sets, (2) examination of the variations in spatial and spectral characteristics of uncontaminated apples, (3) exploring differences between fecal and apple spectra by amount of feces applied, and (4) keeping the image–processing algorithms simple to allow for real–time image analyses. To allow

analyses of only the contaminated and uncontaminated areas of apple surfaces, a simple threshold applied to red fluorescence band images (685 nm) was used to create a mask for each individual apple. The threshold value was determined visually for each cultivar.

Two approaches were used initially to reduce the complexity of hyperspectral data sets. First, spectral bands for analyses were selected based on the emission maxima of apples and feces (e.g., Heisel et al., 1997; Kim et al., 2001a; Kim et al., 2001c). Individual fluorescence emission bands (maxima) of the contaminated and normal sample surfaces were contrasted to study the effects of spatial variations within a wavelength and across spectral responses. Additional transformations tested to discriminate fecal contamination over the range of normal apple surfaces were combinations of two band ratio images using the four emission maxima. Second, entire data sets were subjected to principal component analyses (PCA) using the ENVI program. Subsequently, individual principal component (PC) images were visually evaluated to determine those PC images with (1) the least variation across uncontaminated sample surfaces and (2) the largest contrast between contaminated spots and sample surfaces. The PC images were also subjected to a simple threshold classification to test discrimination of fecal–contaminated areas from uncontaminated apple surfaces. As each PC image is a linear sum of images at individual wavelengths multiplied by corresponding (spectral) weighing coefficients, the wavelengths with the highest weighing coefficients represent the dominant (significant) wavelengths. Images at the several identified wavelengths were subjected to PCA again along with the band ratios of fluorescence emission maxima as multispectral approaches for discrimination of fecal–contaminated areas from normal apple surfaces.

Results and Discussion

Hyperspectral Fluorescence Images

Figure 1 shows gray–scale fluorescence images of Red Delicious apples at 450 (F450), 530 (F530), 685 (F685), and 735 (F735) nm obtained from hyperspectral fluorescence images. For presentation purposes, the images were linearly stretched to achieve optimal visual contrast. These emission bands were selected to represent fluorescence emission maxima for the blue, green, red, and far–red regions of the spectrum for plant materials. The adjacent graphs of RFI

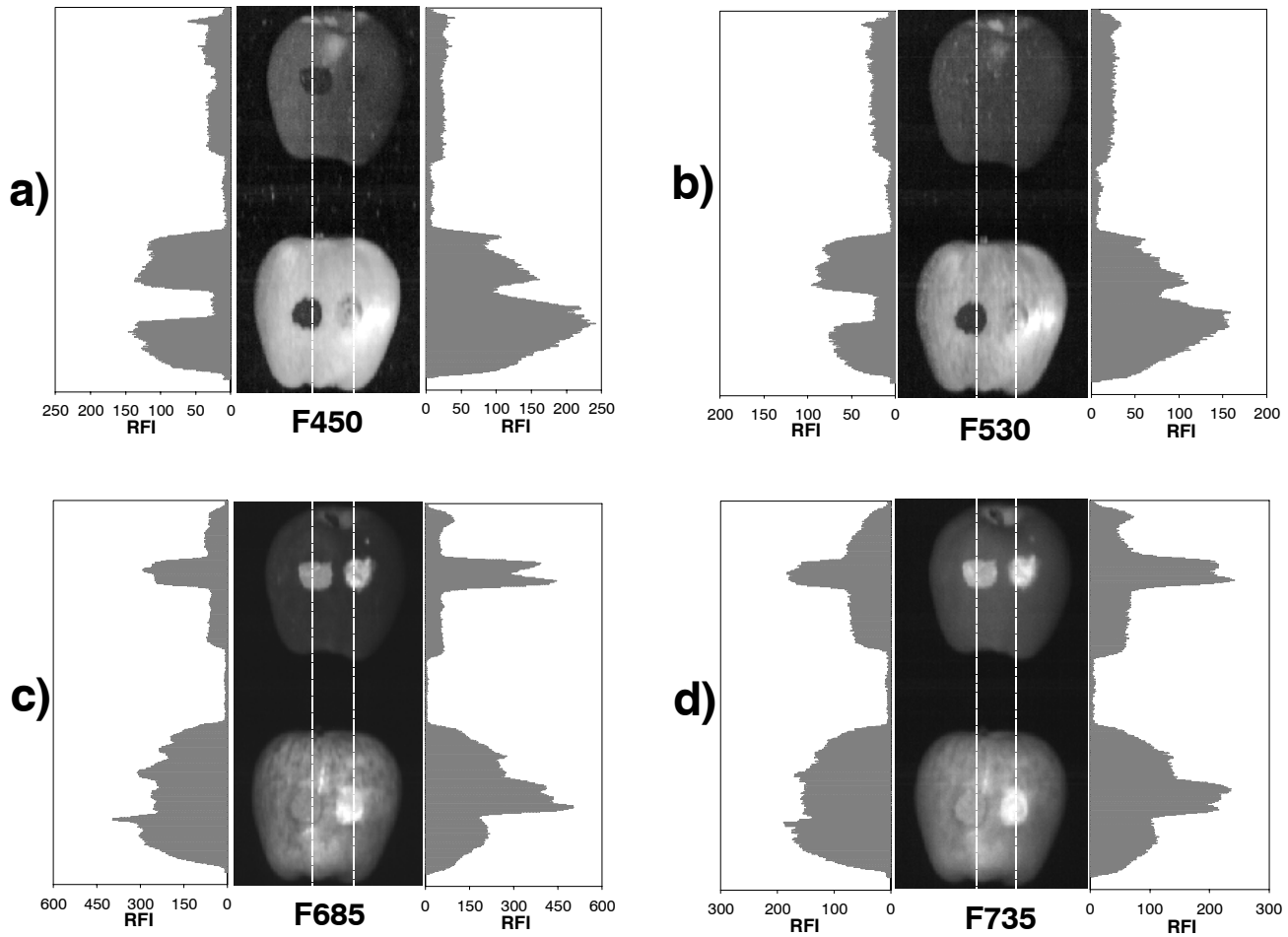

Figure 1. Gray–scale images of Red Delicious apples at 450, 530, 685, and 735 nm. For each set of images (a–d), the top apple is sun–exposed (uniform red color) and the bottom apple is shaded (variegated red and green coloration). The graphs of RFI correspond to the adjacent dotted lines. Note that the graphs transect both the thick (left side) and thin (right side) feces–treated spots. Images were acquired with four apples, but only two apples (sun–exposed and shaded) are shown.

values illustrate normal variation on intensities across uncontaminated apple surfaces as well as responses due to feces application.

The shaded apples exhibited higher RFI at all four wavelengths compared to the sun–exposed apples. This difference is probably indicative of higher contents of fluorophores, such as chlorophyll *a*, in the shaded apples. As apples ripen, there is a concomitant degradation of chlorophyll *a*. Fluorescence emissions for a multi–compound biological system such as apples result from complex biophysical and biochemical interactions of many factors. The lower RFI observed for the sun–exposed apples compared to the shaded apples may also emanate from higher accumulation of UV protection compounds such as flavonols. It has been reported that flavonol species compete for UV excitation energy, and hence mitigate fluorescence emissions from plant materials (Kim et al., 1998).

The spatial RFI profiles showed lower variation for uncontaminated surfaces of sun–exposed apples as compared to the shaded apples. The profiles also demonstrated similarities between F450 and F530, and F685 and F735, images in terms of RFI changes. In contrast, the F450 and F530 profiles were markedly different from the F685 and F735 profiles. These observations provide further evidence that compounds other than chlorophyll *a* are responsible for F450 and F530 emissions.

The F685 and F735 images reveal that the thin fecal smears, which are not readily visible to the human eye, are easily discernable due to high (bright) RFIs. This finding suggests that fluorescence may provide a sensitive basis for detection of fecal contamination. The thin feces spot was also apparent on the shaded apple in the F450 and F530 images, and the RFIs for the spot were lower compared to the surrounding, uncontaminated, apples surfaces. However, the thin spot was not visible on the sun–exposed apple, and the RFIs were similar for both uncontaminated and contaminated surfaces. In addition, the thin feces spot on the shaded apple in the F450 and F530 images showed higher emissions compared to the similar spot on the sun–exposed apple, due presumably to background effects related to the relatively higher emissions from uncontaminated areas of the shaded apple. In contrast, the thin feces spots on the shaded and sun–exposed apples in the F685 and F735 images showed approximately equal emission intensities, suggesting less influence of background emissions. For the thick feces spots, RFIs in the F450 and F530 images were lower than or equal to those for uncontaminated surfaces, while at F685 and F735, RFIs were higher than or equal to those for uncontaminated surfaces. Overall, the thin feces spots exhibited higher RFIs compared to the thick feces spots. This difference was probably due to the thick feces having higher moisture content compared to the thin smears. In general, because of the heterogeneous fluorescence intensities from uncontaminated apple surfaces and the variability in fluorescence responses of feces relative to the thickness of the applied feces, single (monochromatic) waveband imaging may not allow for reliable detection of fecal contamination. For the other cultivars, RFI differences between sun–exposed and shaded sides were not as great as for Red Delicious apples, and images for these cultivars are not presented for brevity.

Fluorescence Emission Spectra

Figure 2 shows representative fluorescence emission spectra for the four apple cultivars including spectra for sun–exposed and shaded sides, and thin and thick feces–treated spots. Apples exhibited four distinctive fluorescence emission maxima in the blue, green, red, and far–red regions of the spectrum when excited with UV radiation. Note that emissions in the green region for Red Delicious were not clearly visible in the figure. Fluorescence emissions from apples were broad in nature with apparent convolution of local emission maxima. This convolution resulted in small shifts of emission maxima, especially for the emission peaks in the green and far–red regions of the spectrum. Observed RFIs from apple surfaces were cultivar dependent, and within each cultivar, shaded apples exhibited higher fluorescence emissions throughout the spectral region compared to sun–exposed apples. Prior to this study, only chlorophyll *a* fluorescence emission characteristics in the red region have been studied (Abbott et al., 1997); the goal was to assess changes in apple quality associated with storage conditions (DeEll et al., 1996). To facilitate potential future studies of apple characteristics, fluorescence emissions from the shaded and sun–exposed sides of individual cultivars at the emission maxima are provided in table 1.

Distinctive chlorophyll *a* fluorescence emissions in the red and far–red regions of the spectrum were observed from all the apples, including those with red coloration. The feces also exhibit spectral emissions with characteristics resembling chlorophyll *a* molecules. Kim et al. (2001a) demonstrated the presence of chlorophyll *a* and its metabolites in several animal feces based on the fluorescence excitation and emission characteristics obtained using a spectrofluorometer. In the blue–green regions, the thin feces spots showed lower emissions compared to respective apple surfaces. In contrast, the thin feces spots showed increased emissions in

Table 1. Mean (n = 4) fluorescence emission intensities of four apple cultivars, shaded and sun–exposed sides, measured with the ISL hyperspectral imaging system at the blue, green, red, and far–red regions of the spectrum with UV (365 nm) excitation. Standard errors are provided in parentheses.

Apple Cultivar		Fluorescence Emission Bands			
		Blue (450 nm)	Green (530 nm)	Red (685 nm)	Far–Red (735 nm)
Fuji	Shaded	286.7 (23.0)	301.0 (13.6)	538.8 (84.7)	247.7 (31.9)
	Sun–exposed	44.8 (5.2)	65.3 (10.7)	112.1 (18.2)	92.4 (4.0)
Gala	Shaded	138.3 (26.9)	169.4 (41.1)	252.4 (35.3)	90.7 (11.9)
	Sun–exposed	74.5 (5.1)	97.4 (8.7)	194.3 (11.9)	85.1 (5.1)
Golden Delicious	Shaded	124.1 (35.9)	187.7 (12.9)	177.9 (37.3)	95.6 (24.3)
	Sun–exposed	63.9 (6.6)	139.9 (18.5)	107.6 (13.9)	62.6 (6.4)
Red Delicious	Shaded	140.6 (10.8)	100.4 (8.4)	231.8 (2.9)	116.0 (6.0)
	Sun–exposed	41.3 (10.0)	35.6 (6.4)	68.9 (8.9)	57.6 (4.6)

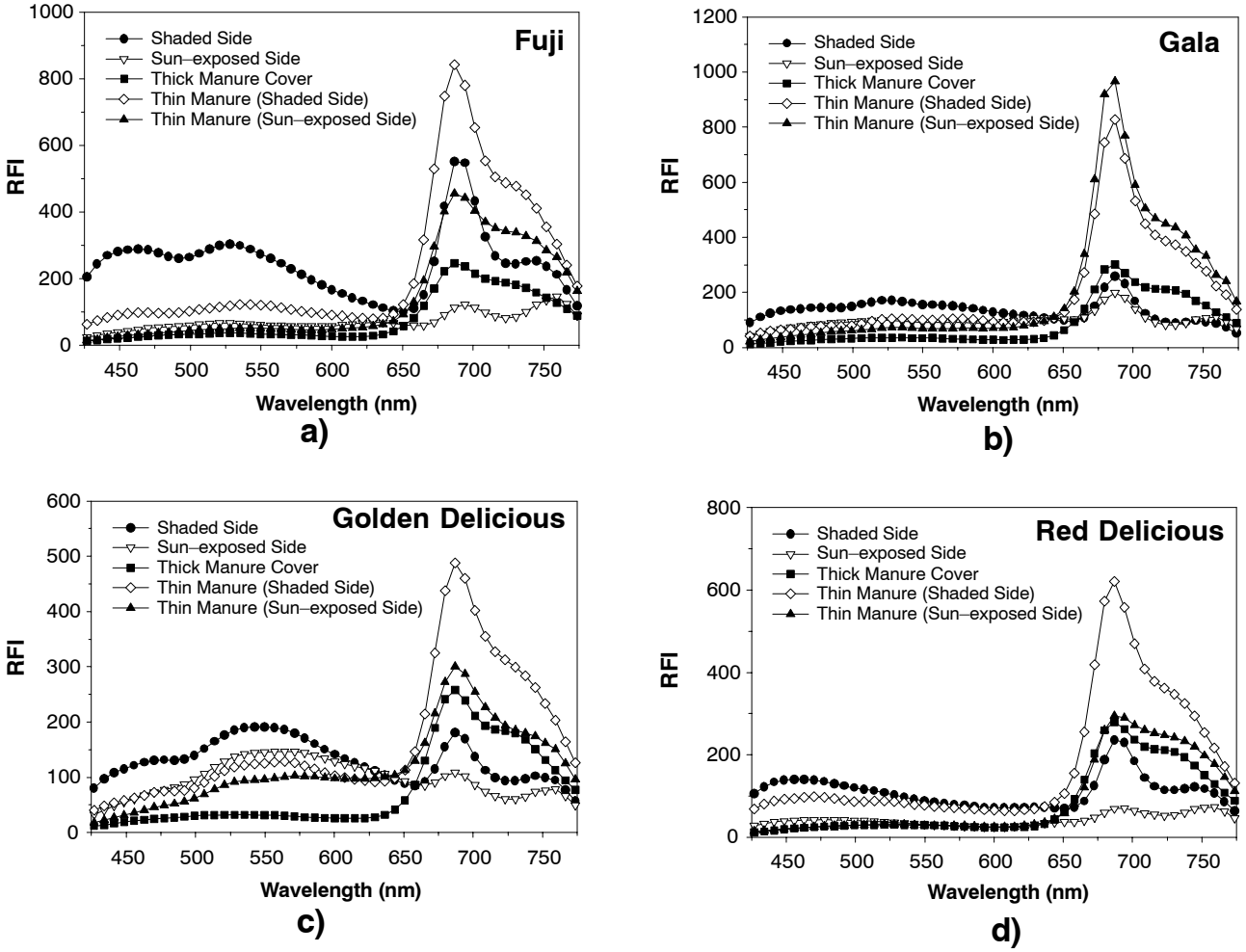

Figure 2. Representative fluorescence emission spectra following UV (365 nm) excitation for the sun–exposed and shaded sides of the four apple cultivars along with responses of spots treated with thick or thin feces. Spectral estimates for fecal–contaminated areas represent the average responses of four rectangular regions of interest, each with an area of 10 × 10 pixels. Estimates for sun–exposed and shaded apple surfaces are based on two regions of interest adjacent to the areas of contamination.

the red and far–red regions regardless of apple colorations. The thick feces treatment produced the lowest emissions in the blue–green regions of the spectrum regardless of the apple cultivar. In the red and far–red regions, the thick feces emissions were higher compared to apple surfaces, except for Fuji apples for which the effect was not as pronounced.

Concurrent evaluation of both fluorescence images and spectra (figs. 1 and 2) provides additional insights into how best to detect fecal contamination on apples. As indicated previously, data from a single emission band may be inadequate to allow successful identification of contaminated areas. However, opposite trends in fluorescence emissions are apparent in the responses of feces–treated spots and apple surfaces in the blue–green vs. red/far–red regions. This opposite trend suggests that multispectral approaches such as band ratios may provide a means to emphasize the spectral differences between the fecal–contaminated and normal apple surfaces (see below).

PCA of Hyperspectral Fluorescence Images

Figure 3 illustrates first through fourth principal component (PC–1 through PC–4) images obtained by PCA of hyperspectral fluorescence images of fecal–contaminated apples based on the entire spectrum region (90 channels) under investigation. The PCA provides a means to reduce the high spectral dimensional of image data. The first principal component image represents a composite of information from all the spectral regions, which accounts for the largest variance. Subsequent PC images are ordered in terms of the sample variance. In general, the PC–2 images showed the greatest contrast between contaminated and uncontaminated surfaces; feces contamination appears as dark spots regardless of the thickness of the applied feces, and the variation in intensities among apple surfaces (within and between apples) was small. This visual assessment was confirmed by applying a simple threshold to the PC–2 images (figure not shown). A cultivar–dependant threshold allowed the best discrimination of the feces–treated spots from uncontaminated apple surfaces regardless of sun–exposure, with one exception. A small fraction of the shaded Fuji surfaces in the PC–2 images had similar brightness intensities as the feces–treated spots. Figure 4 illustrates weighing coefficients for the PC–2 images by cultivar. The dominant spectral regions approximately coincided with the fluorescence emission maxima from the sample materials. This observation is a further indication that the fluorescence emission maxima may be the optimal spectral bands for the discrimination of fecal–contaminated spots from uncontaminated apple surfaces.

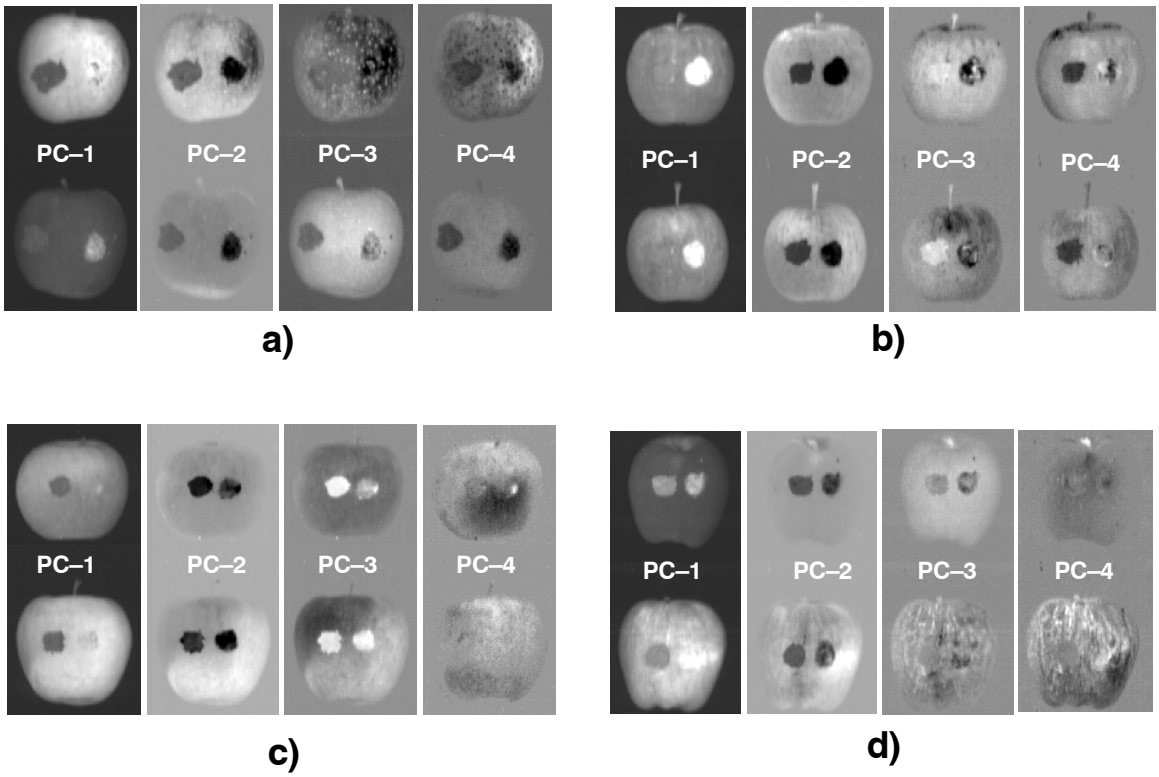

Figure 3. First (PC–1) through fourth (PC–4) principal component images for (a) Fuji, (b) Gala, (c) Golden Delicious, and (d) Red Delicious apples. For each cultivar, the top apple is sun–exposed and the bottom apple is shaded (for Fuji, the top apple is shaded and the bottom apple is sun–exposed). PCA of the original hyperspectral fluorescence images were based on the entire spectrum region (90 channels) under investigation. Note that images were acquired with four apples, but only two apples per cultivar (sun–exposed and shaded) are shown.

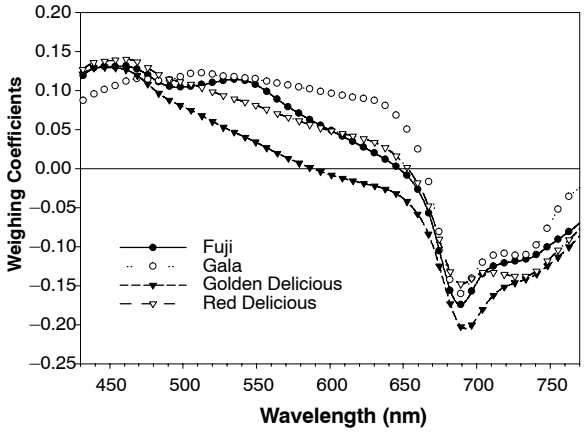

Figure 4. Weighing coefficients for the second principle component (PC–2) images by cultivar. Note that the dominant spectral regions approximately coincided with the fluorescence emission maxima from the sample materials.

PCA Based on Multispectral Fluorescence Emission Maxima

To further investigate the use of fluorescence emission maxima for multispectral algorithms, PCA was performed based on the individual images at 450, 530, 685, and 735 nm. The benefit of restricting analyses to a limited number of spectral regions is that the results can be used to define an appropriate multispectral algorithm for the detection of fecal contamination of apples. Figure 5 illustrates the first through third principal component (PC–1 through PC–3) images obtained by PCA based on the four spectral regions identified above (450, 530, 685, and 735 nm). The resultant multispectral–based PC images were similar in appearance to the PC images previously obtained based on analyses of 90 spectral regions (fig. 3). The multispectral PC–2 images provided clear visual distinctions between the fecal treatments and the uncontaminated apple surfaces, with one exception. Portions of the uncontaminated, sun–exposed Fuji apples appeared by visual analysis to be similar to the contaminated areas, and a simple threshold could not differentiate between these areas and the contaminated areas.

Band Ratio Images

All possible band ratio images for Red Delicious apples based on the four identified multi–spectral bands are shown in figure 6a. The F530/F450 and F685/F735 ratios were ineffective in producing images for distinguishing the fecal–contaminated spots from uncontaminated apple surfaces. The other four ratio images improved discrimination compared to individual band images, and the F685/F450 image resulted in the best image such that the fecal–contaminated spots are significantly different from the uncontaminated apple surfaces with relatively small spatial variation for normal apple surfaces. The effective delineation of the feces spots from the apple surfaces by these four ratio images was by virtue of the fecal samples having equal to lower RFIs in the blue and green regions, along with equal to higher RFIs in the red and far–red regions, when compared to the uncontaminated apple surfaces. Representative F685/F450 images for the other cultivars are shown in figure 6b. Note that these images also demonstrated the clear differences between the fecal–contaminated and uncontaminated apple surfaces regardless of the thickness of the feces treatments.

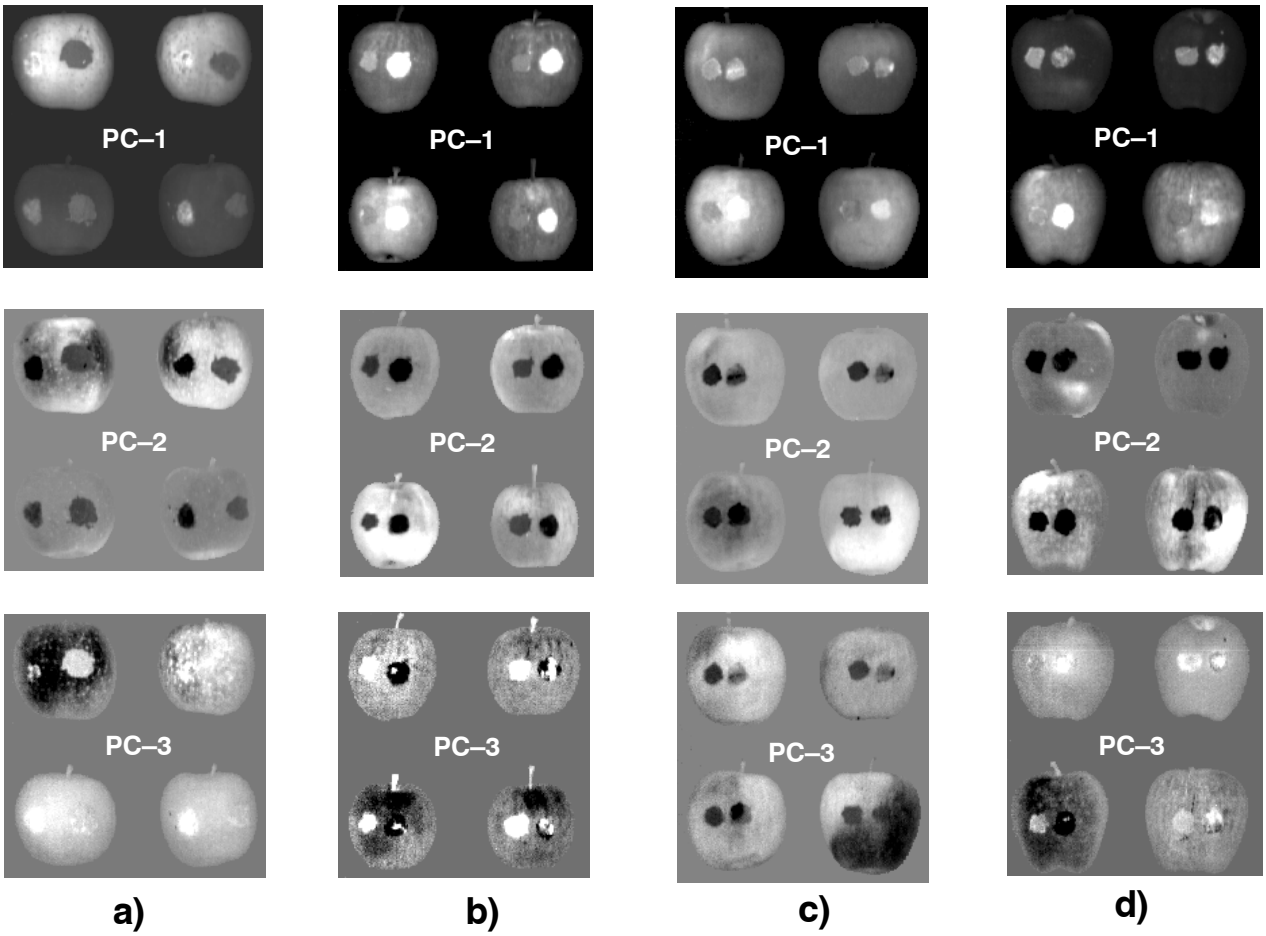

Figure 5. First (PC–1) through third (PC–3) principal component images for (a) Fuji, (b) Gala, (c) Golden Delicious, and (d) Red Delicious apples. For each cultivar, the top apples are sun–exposed and the bottom apples are shaded, except for Fuji. PCA were based on four spectral bands: 450, 530, 685, and 735 nm.

Practical Considerations

This investigation demonstrated that hyperspectral fluorescence imaging techniques can be used to define several optimal bands for discriminating fecal–contaminated areas from uncontaminated apple surfaces. Applying a simple threshold to band ratio images of two identified bands (e.g., F685/F450) allowed detection of fecal contamination on all apples tested. In contrast, in a companion study, in which VIS/NIR reflectance methods were used to examine the same contaminated apples, only a fraction of the thin feces spots could be discriminated from the normal apples surfaces with the use of a simple threshold.

Auto–fluorescence (quantum yield) from fecal matter is relatively low. Thus, to implement fluorescence techniques on–line requires either a dark environment to eliminate ambient and stray light, or a pulsed light source coupled with a gated–detection system. With the use of a pulsed excitation source, such as a laser, in conjunction with a gated–intensified imaging device, detection of multispectral fluorescence emissions from biological entities is feasible in the presence of ambient radiation; several articles describe the use of laser–induced fluorescence techniques in the field (Kim et al., 1973; Hoge et al., 1983; Cecchi et al., 1994). Furthermore, a common aperture multispectral lens adapter can be used to capture fluorescence emissions excited by an expanded laser beam at up to four emission bands (Chen et al., 2002). Figure 7 illustrates such a system developed in our laboratory. In addition, it has been suggested that detection of fecal contamination on agricultural commodities can be improved by proper selection of excitation wavelengths (Kim et al., 2001a). Results from this prior study suggest that results in the current study could have been improved by using an excitation wavelength around 410 to 420 nm.

Conclusions

The results of this investigation indicate that multispectral fluorescence techniques can be used to effectively detect fecal contamination on apple surfaces. Because of the limited sample size, delineation of the optimal detection scheme is beyond the scope of the current study. However, both principal component analysis and examination of emission maxima identified the same four multispectral bands centered at 450, 530, 685, 735 nm as being the optimal bands to allow discrimination of contaminated apple surfaces. Furthermore, simple two–band ratios using two of these four bands were found to reduce the variations in normal apple surfaces while accentuating differences between contaminated and uncontaminated areas. These results suggest that use of multispectral fluorescence techniques for detection of fecal contamination on apples in a commercial setting may be feasible.

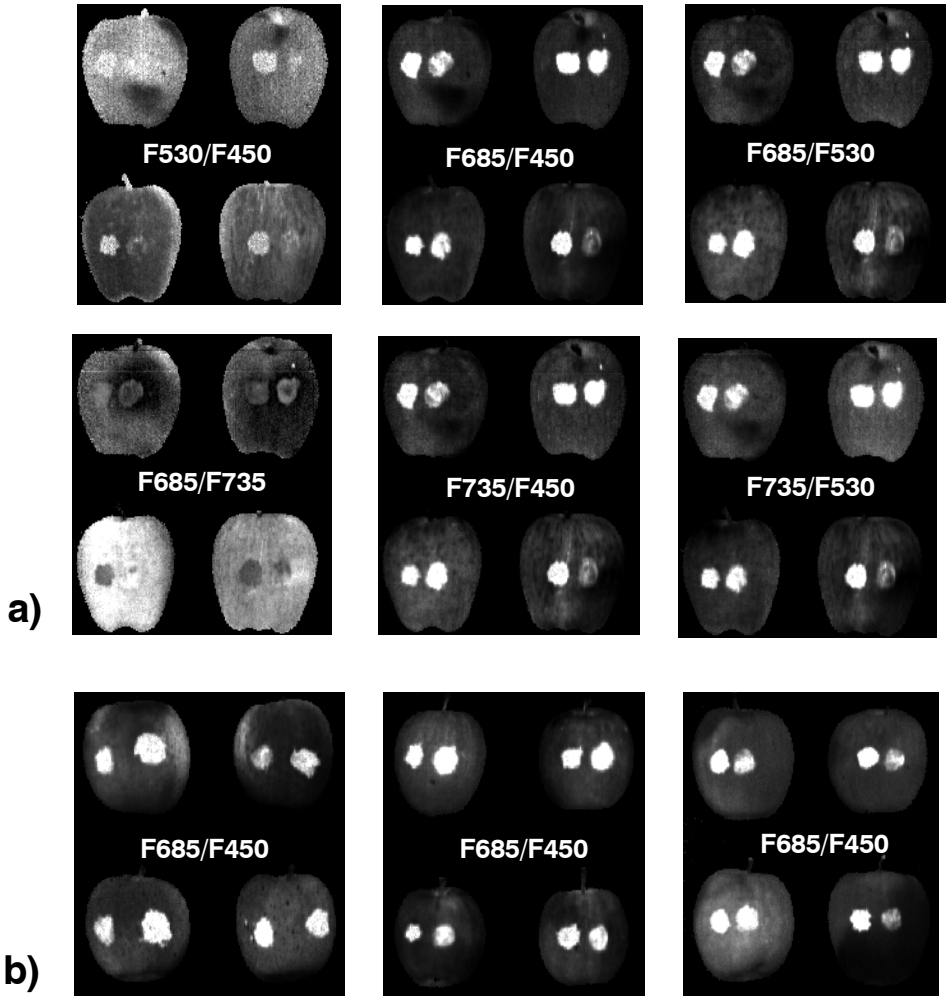

Figure 6. Comparison of band ratio images for Red Delicious apples (a) demonstrating that the ratio of either red or far–red to the blue or green bands reduces variation in uncontaminated surfaces while accentuating the difference between contaminated and uncontaminated surfaces. Representative F685/F450 ratio images are shown (b) for Fuji, Gala, and Golden Delicious apples (left to right).

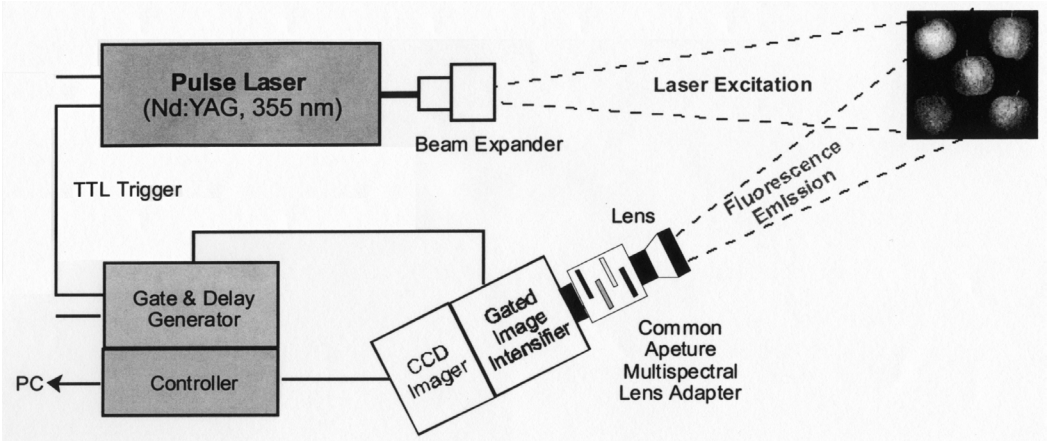

Figure 7. Schematic diagram, including critical components of a multispectral laser–induced fluorescence imaging system.

REFERENCES

Abbott, J. A., R. Lu, B. L. Upchurch, and R. L. Stroshine. 1997. Technologies for non–destructive quality evaluation of fruits and vegetables. *Horticultural Reviews* 20: 1–20.

Cecchi, G., M. Bazzani, V. Raimond, and L. Pantani, 1994. Fluorescence LIDAR in vegetation remote sensing: System features and multiplatform operation. *IGARSS '94 Digest* 1: 637–639.

Chappelle, E. W., J. E. McMurtrey, and M. S. Kim. 1991. Identification of the pigment responsible for the blue

fluorescence band in laser–induced fluorescence (LIF) spectra of green plants, and the potential use of this band in remotely estimating rates of photosynthesis. *Remote Sens. Environ.* 36: 213–218.

Chen, Y. R., K. Chao, and M. S. Kim. 2002. Future trends of machine vision technology for agricultural applications. *Comp. Elec. in Agric.* 36(2–3): 173–191.

Cody, S. H., M. K. Glynn, J. A. Farrar, K. L. Cairns, P. M. Griffin, J. Kobayashi, M. Fyfe, R. Hoffman, A. S. King, J. H. Lewis, B. Swaminathan, R. G. Bryant, and D. J. Vugia. 1999. An outbreak of *Escherichia coli* O157:H7 infection from unpasteurized commercial apple juice. *Annals of Internal Med.* 130: 202–209.

DeEll, J. R, R. K. Prange, and D. P. Murr. 1996. Chlorophyll fluorescence of Delicious apples at harvest as a potential predictor of superficial scald development during storage. *Postharvest Biol. Technol.* 9: 1–6.

FDA. 2001. Hazard analysis and critical control point (HAACP): Procedures for the safe and sanitary processing and importing of juices. *Federal Registry* 66(13): 6137–6202.

Harris, P. J., and R. D. Hartley. 1976. Detection of bound ferulic acid in cell walls of the Gramineae by ultraviolet fluorescence microscopy. *Nature* 259: 508–510.

Hewett, J., V. Nadeau, J. Ferguson, H. Moseley, S. Ibbotson, J. W. Allen, W. Sibbett, and M. Padgett. 2001. The application of a compact multispectral imaging system with integrated excitation source to *in vivo* monitoring of fluorescence during topical photodynamic therapy of superficial skin cancers. *Photochem. Photobiol.* 73(3): 278–282.

Hoge, F. E., R. N. Swift, and J. K. Yungel. 1983. Feasibility of airborne detection of laser–induced fluorescence from green plants. *Applied Optics* 22: 2991–2998.

Kim, H. H. 1973. New algae mapping technique by the use of an airborne laser fluoresensor. *Applied Optics* 12: 1454–1459.

Kim, M. S., E. H. Lee, C. L. Mulchi, J. E. McMurtrey, E. W. Chappelle, and R. A. Rowland. 1998. Fluorescence imaging of soybean flavonol isolines. *SPIE* 3382: 170–178.

Kim, M. S., A. M. Lefcourt, and Y. R. Chen. 2001a. Determination of optimal fluorescence bands for detection of fecal contamination on agricultural commodities. *J. Food Prot.* (in submission).

Kim, M. S., J. E. McMurtrey, C. L. Mulchi, C. S. T. Daughtry, E. W. Chappelle, and Y. R. Chen. 2001b. Steady–state multispectral fluorescence imaging system for plant leaves. *Applied Optics* 40: 157–166.

Kim, M. S., Y. R. Chen, and P. M. Mehl. 2001c. Hyperspectral reflectance and fluorescence imaging system for food quality and safety. *Trans. ASAE* 44(3): 721–729.

Krizek, D., E. M. Middleton, R. Sandhu, and M. S. Kim. 2001. Evaluating UV–B effects and EDU protection in cucumber leaves using fluorescence images and fluorescence emission spectra. *J. Plant Physiol.* 158(1): 41–53.

Sowinska, M., T. Decker, C. Eckert, F. Heisel, R. Valcke, and J. Miehe. 1998. Evaluation of nitrogen fertilization effect on apple–tree leaves and fruit by fluorescence imaging. *Proc. SPIE* 3382: 100–111.

Tassetti, V., A. Hajri, M. Sowinska, S. Evrard, F. Heisel, L. Q. Cheng, J. A. Mieh, J. Marescaux, and M. Aprahamian. 1997. *In vivo* laser–induced fluorescence imaging of a rat pancreatic cancer with phophorbide–*a*. *Photochem. Photobiol.* 65(6): 997–1006.

Throop, J. A., D. J. Aneshansley, and B. L. Upchurch. 1995. An image processing algorithm to find new and old bruises. *Applied Eng. in Agric.* 11(5): 751–757.